Available online at www.sciencedirect.com
ScienceDirect
Journal of Sound and Vibration 308 (2007) 815–830
JOURNAL OF SOUND AND VIBRATION
www.elsevier.com/locate/jsvi

Experiments and simulations on ultrasonically assisted drilling

P.N.H. Thomas*, V.I. Babitsky

Wolfson School of Mechanical and Manufacturing Engineering, Loughborough University, UK

Accepted 26 March 2007
The peer review of this article was organised by the Guest Editor
Available online 30 May 2007

Abstract

Ultrasonically assisted drilling (UAD) has received great interest in the past few years by both academia and industry. The technology has already demonstrated a multitude of advantages over conventional drilling technology although its use has been mainly thwarted by inconsistent results. In order to aid the further development of UAD, a better understanding of the underlying dynamical process is required. In this work, an investigation into UAD is performed. Longitudinal vibration is used to excite standard 8 mm high-speed steel drill bits and mild steel samples are used for cutting tests. A swept sine wave is used to excite the system whilst the cutting forces that result are acquired. Clearly optimal regions are revealed and these are discussed. Subsequent to the experimental investigation, three-dimensional finite element drill bit models are employed to further understand the drill bit's vibrational characteristic. The simulation results show new areas of interest in which further work is necessitated.

1. Introduction

Drills, as basic hole-producing tools have existed in nearly all civilisations for which there is a recorded history. The first machine made twist drills were not produced until about 1860, and the first truly modern twist drills began with the invention of high-speed steel in around 1900 [1].

Of all the machining processes currently performed in manufacturing, drilling accounts for about 25%, and one estimate states that US manufacturing companies are consuming 250 million twist drills per year [2].

Twist drills and hole producing devices are constantly being developed and fine tuned. The standard layout of the twist drill, however, has evolved over time and has become universally accepted.

Important drill bit characteristics include the torque and thrust required for drilling, the life of the drill bit, the rate of material removal, hole positional accuracy, and the quality of the hole produced. Factors that affect these characteristics include the drill's geometry, the workpiece's material, the drill bit's material (including coating), cutting speeds/feed rates, and any coolant/lubrication employed.

Vibratory motion, at audible and low frequencies, has previously been applied to conventional drill bits revealing some favourable results [3–5]. This work, however, regards the application of ultrasonic vibration

*Corresponding author. Tel.: +44 7961 907319.
E-mail addresses: P.N.H.Thomas@lboro.ac.uk (P.N.H. Thomas), V.I.Babitsky@lboro.ac.uk (V.I. Babitsky).

0022-460X/$ - see front matter © 2007 Elsevier Ltd. All rights reserved.
doi:10.1016/j.jsv.2007.03.081

(i.e. above the audible frequency range) to modify the conventional twist drilling process in to that of ultrasonically assisted drilling (UAD).

There are many documented advantages of UAD. These include a reduced drilling reaction force and torque (in addition to energy savings, this allows thin structures to be drilled without deformation) [6,7], increased positional accuracy (especially when drilling on an incline) [8,9], reduced or eliminated burr formation [7,10–12], significantly improved chip expulsion (allowing deeper holes to be drilled) [8,13–15], an improvement in both hole roundness and size [8,16], extended drill bit life [14,16–18], increased material removal rate [19–21], improved hole surface finish [8,13,22,23], and a reduced or eliminated built up edge [13,22]. Experiments and computer simulations previously performed at Loughborough University with regards to turning operations (which are directly applicable to UAD) have also indicated that the use of ultrasonic vibration significantly reduces the work hardening of workpiece materials as they are cut [24–26].

The number of manufacturing steps required to form components can be reduced as a result of the advantages detailed e.g. no de-burring operations are required, no spot drilling operation would be required when drilling into an inclined surface, improvements in hole quality remove the need for a subsequent reaming operation, etc. Application specific advantages also include reduced delamination when drilling layered structures [23,27], reduced fibre pullout when drilling fibrous materials [7], reduced exit hole cratering when drilling hard and brittle materials (discovered during tests at Loughborough University), and reduced chipping and cracking when drilling hard, brittle materials (discovered during tests at Loughborough University).

Ultrasonic vibration can be applied to a twist drill in several ways. Purely longitudinal vibration can be applied i.e. along the axis of the twist drill as shown in Fig. 1a, purely torsional vibration can be applied i.e. the drill bit can be twisted in a reciprocating motion as shown in Fig. 1b, or a combined longitudinal/torsional motion can be applied. Alternative excitation methods also exist such as applying ultrasonic excitation to the coolant as it is conveyed to the cutting zone [28]. The coolant thus acts as a waveguide and essentially facilitates the agitation and conveyance of the cutting fluid within the cutting zone. Another method is to apply ultrasonic vibration to the workpiece. Work has been conducted in this area, both in directions which coincide with the drill bit's axis [7,11,15], and in a plane that is perpendicular to the drill bit's axis [29]. Both of these excitation methods have proven advantageous.

Initial UAD experiments were conducted in the early 1950s [6,30,31]. Interest in UAD technology has persisted over time and has recently been the subject of several works [11,17,22]. Research is ongoing both at Loughborough University and at other organisations [32]. The application of UAD for forming extremely small or microholes has also been investigated with very positive results [8,33,34].

Several companies have investigated the use of UAD [10,15,35], and commercially available UAD drilling systems have been developed [36–38]. Much of the research conducted on UAD duplicates previous results, and has painted a rather inconsistent picture with respect to the results obtained [30,38]. This is mostly due to the lack of understanding behind the process. The technology has been employed industrially, but never on a large scale [15,20,37–39].

The disadvantages of UAD include the cost of the equipment required, the sometimes unpredictable results obtained with its use (due to the process being misunderstood), and some investigations have found that

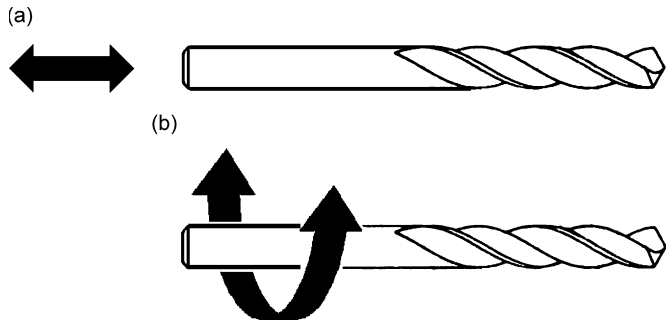

Fig. 1. Drill bit excitation: (a) longitudinal excitation, (b) torsional excitation.

although the cutting edges of the drill bits employed are utilised more evenly, chipping can occur which prematurely ends the drill bit's life [11] (this effect has also been encountered at Loughborough University on uncoated drill bits). These disadvantages can be effectively overcome through the proper understanding of the process and the development of a dependable and commercially viable system.

The viewpoint of the majority of the authors documenting the development of UAD is that of one-dimensional vibration; be it longitudinal or torsional. A purely kinematic model of UAD has been derived [16], but this does not include the influence of the reactive drilling forces on the motion of the vibrating system, and only considers longitudinal vibration (i.e. one dimensional). The influence of the drilling reactive loads on the motion of the drill bit has been investigated in one dimension [40] from the viewpoint of maximising the vibration present, but no fully three-dimensional dynamic model has yet been created (as far as the authors are aware).

This work endeavours to understand the dynamic process that occurs during UAD and highlight areas that require further improvement. This is achieved both experimentally, and with the use of numerical finite element (FE) computer models.

2. Experimental set-up and methodology

To further investigate UAD, a standard Langevin-type bolt clamped ultrasonic transducer operating in a longitudinal vibration mode was designed (Fig. 2), fabricated and mounted into a universal lathe's chuck via a suitable adaptor (see Fig. 3). As such, the transducer, in which was mounted a standard 8 mm high speed steel (HSS) 'Jobber' twist drill (Fig. 3), could be rotated and fed into the workpieces under test. This arrangement also facilitated stationary analysis of the vibration exhibited by the ultrasonic system. The electrical power required to excite the ultrasonic transducer was fed to the transducer via a slip-ring arrangement (Fig. 4) and the transducer was mounted into the adaptor by clamping it at a point of minimal vibration (the shaded ring next to the step in Fig. 2) in order to isolate the machine tool from ultrasonic vibration and maintain a large vibration amplitude in the transducer.

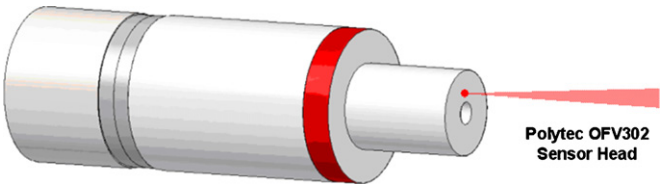

Fig. 2. Ultrasonic transducer design including clamping and measurement positions.

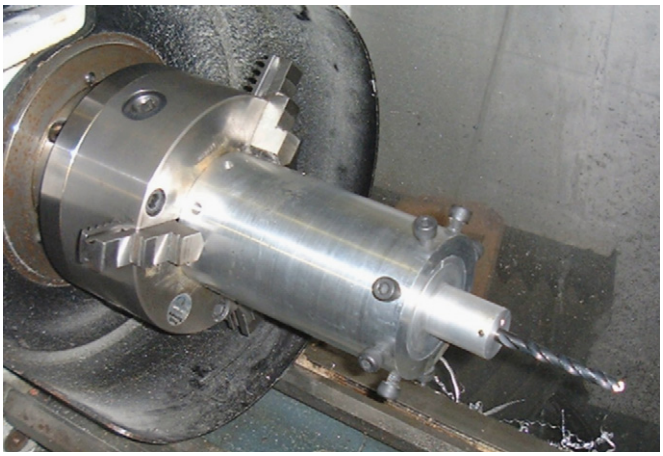

Fig. 3. Longitudinal transducer mounted in a universal lathe.

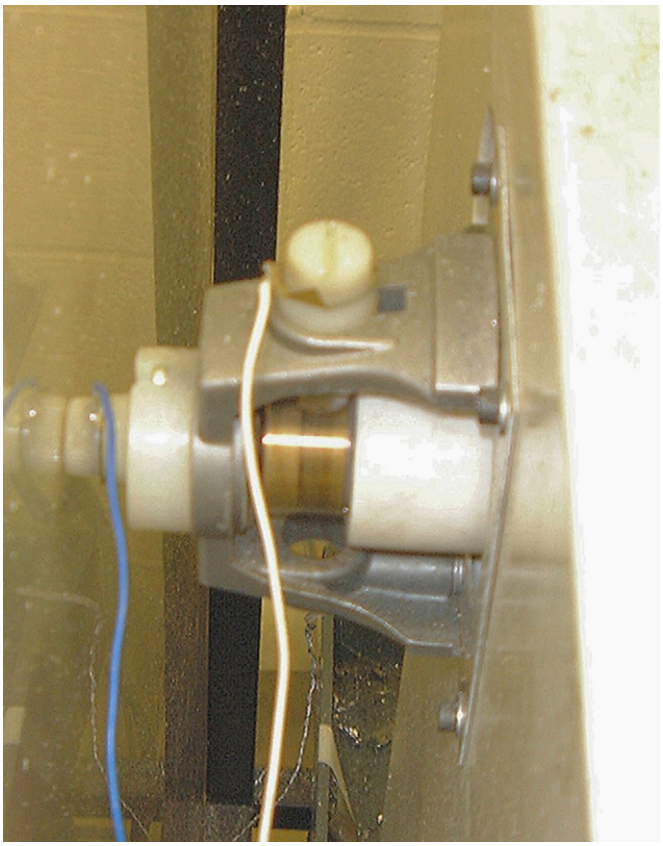

Fig. 4. The slip-ring arrangement used to feed electrical power to the ultrasonic transducer.

2.1. Free vibration testing

In order to obtain an overview of the implications of applying ultrasonic vibration at a specific frequency (as is the case during UAD), a swept sine wave was used to slowly sweep the dynamic system through a range of excitation frequencies. The arrangement of the electrical equipment used to perform this test is shown in Fig. 5. The Black Star signal generator was used to generate a slowly varying saw tooth wave that was inputted into the HP function generator's voltage controlled oscillator (VCO) port. The generator's VCO function allows the frequency generated by the generator to be varied linearly (as opposed to logarithmically) with respect to the voltage inputted. As such, a swept sine wave was generated which was adjusted to slowly vary, within pre-selected frequency ranges, with time. This signal was amplified using a universal amplifier (which has a flat response in the frequency region under investigation), conditioned using a universal matching box, and conveyed to the ultrasonic transducer via the slip-ring arrangement detailed above. The matching box contains a transformer to step the voltage up to that required by the ultrasonic transducer, it also contains an inductor to shunt the capacitance of the piezoelectric elements employed in the transducer. The velocity at strategic positions on the vibrating system was measured using a Polytec Laser Vibrometer, which is a non-contact instrument. The signals generated were captured using a LeCroy Digital Data-recording oscilloscope and transferred to a personal computer (PC) for subsequent processing.

The velocity at the end of the ultrasonic transducer was measured in the position shown in Fig. 2 by the shaded spot. The shaded triangle stemming from this spot shows the path of the laser's beam, which was aligned axially with the transducer. This position was chosen so as to be close to the point at which the drill bit was attached, and was held constant to ensure the consistency of the data obtained. Swept frequency trials were conducted in which the frequency was swept both upwards and downwards both with and without the drill bit attached to the transducer.

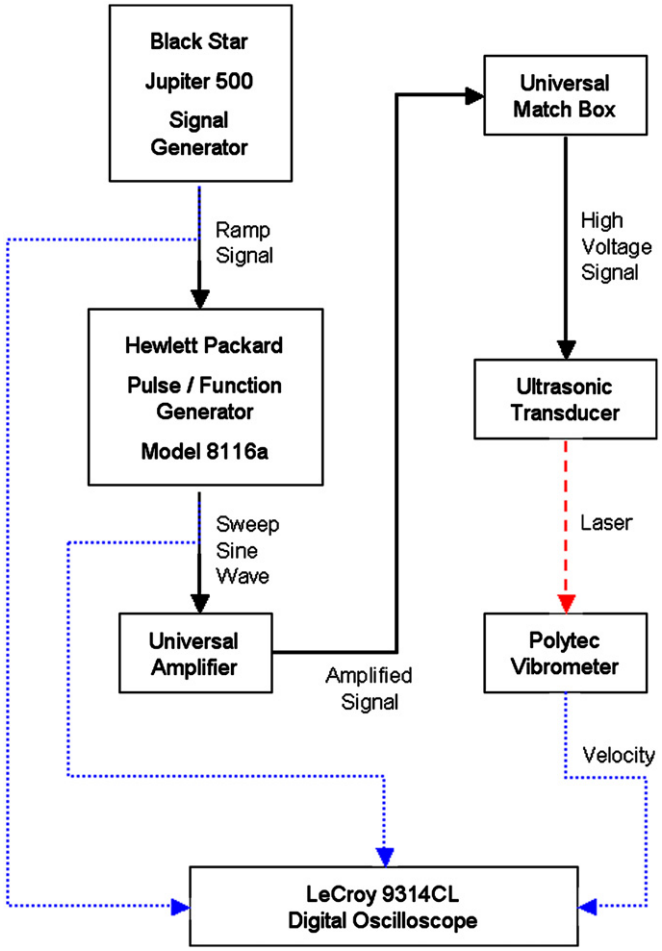

Fig. 5. Electrical arrangement for free vibration testing.

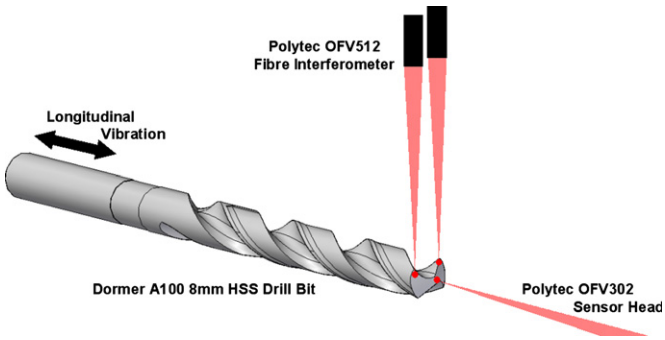

Fig. 6. Measurement of drill bit's longitudinal and torsional vibration.

Subsequent to the free vibration trials conducted on the transducer, the measuring position of the laser vibrometer was moved to the tip of the drill bit (measuring longitudinal vibration), and a second, dual beam, differential-mode vibrometer was used to measure the torsional displacement at the tip of the drill bit. The vibrometers' arrangement is shown in Fig. 6. Again, shaded spots are used to indicate the measurement

positions. The differential-mode vibrometer was employed in order to remove the influence of lateral or bending motion from the data recorded. Again, the frequency was swept both upwards and downwards and the data was recorded as previously.

The magnitude of the electrical voltage supplied by the amplifier was maintained constant during all free vibration experiments apart from in the last experiment (measuring the response of the drill bit's tip) in which the system's excitation amplitude was reduced in order to assist with data capture (due to the level of vibration; the laser vibrometers' signals were found to be discontinuous).

2.2. Drilling reaction force and torque measurement

The reaction force and torque generated during drilling at different frequencies of excitation were obtained using the experimental arrangement shown in Fig. 7. A three-jaw chuck was mounted on a Kistler two-component (thrust and torque) Dynamometer (Type 9271A), which was in turn rigidly attached to the cross-slide of the universal lathe employed for the experiments. The samples under test were clamped in this chuck and had been previously faced and centred to ensure consistent results. The whole arrangement was aligned concentrically and the positional accuracy of the components was monitored throughout the experimental investigation. The transducer/drill bit system remained as described in the previous section.

Fig. 8 shows the electrical arrangement of the equipment used to perform these experiments. It is as for the free vibration test, but due to the drill bit's cutting tip being inside the workpiece, and due to the rotation of the system, no velocity measurements could be taken. Instead, the force and torque signals generated by the Kistler dynamometer were conditioned using Kistler charge amplifiers and again, the signals were captured using the LeCroy oscilloscope and transferred to the PC for subsequent processing.

For these initial trials (as the ultrasonic system had in no way been optimised) a relatively low cutting speed of 370 rev/min was selected, and the recommended feed rate of 0.1 mm/rev was used. All workpiece samples were EN1A; mild steel. This material was chosen as it is tougher than Aluminium (i.e. is closer in nature to stronger materials such as titanium, etc.), relatively easy to machine, cheap, and readily available. All drilling experiments were conducted dry i.e. no lubricant/coolant was employed.

Prior to UAD trials, the dynamometer was calibrated and determined to be accurate and linear in response to both forms of loading (torsional and axial). Drilling trials were also performed under conventional conditions (no ultrasonic excitation) to provide a base line to which to compare the UAD results.

UAD experiments were performed with the frequency of excitation being swept both upwards and downwards.

Many experiments were performed in order that the data obtained could be averaged to give representative results. A new drill bit was used for each test to enable direct comparisons to be made in both the drilling reaction forces generated, and the wear that the drill bits were subjected to.

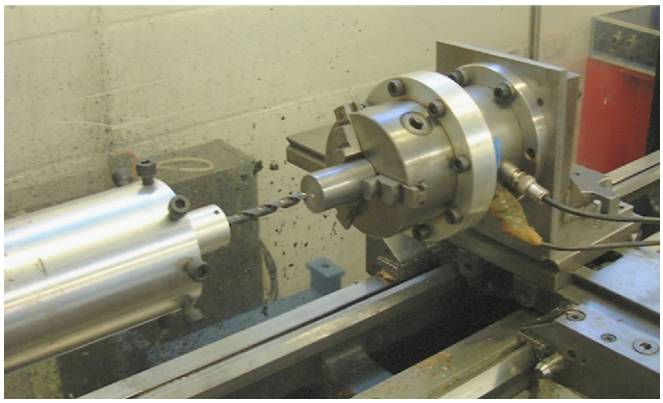

Fig. 7. Experimental arrangement for drilling reaction force/torque measurement.

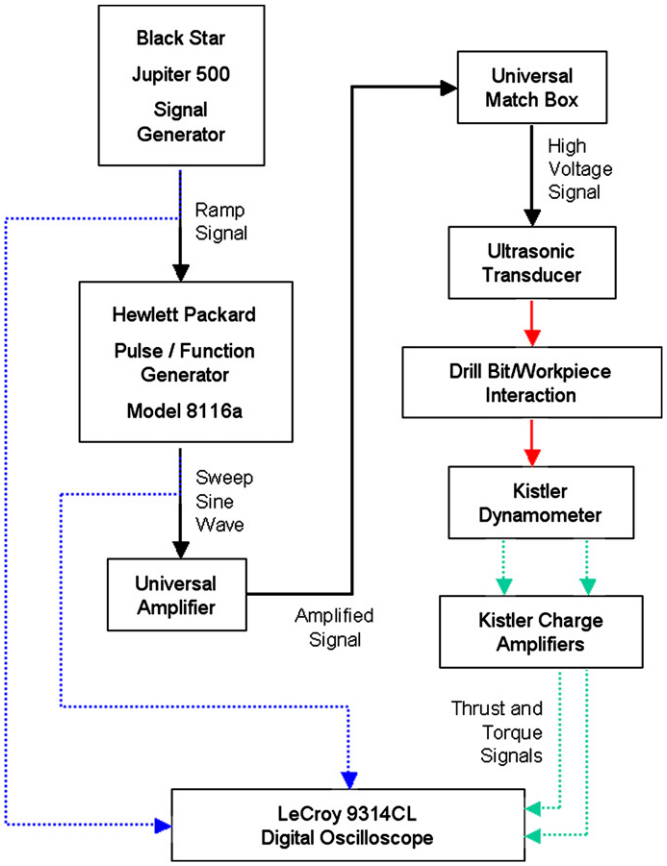

Fig. 8. Electrical arrangement for drilling reaction force/torque measurement.

3. Experimental results and discussion

The experimental results were obtained and analysed in Loughborough University's lab that is devoted to the development of ultrasonically assisted machining technology.

3.1. Free vibration testing

Free vibration experiments were run initially, as described in the previous section, with the transducer only (i.e. no drill bit was attached). The velocity was recorded (in the position shown in Fig. 2 by the shaded spot) at a minimum rate of 20 samples/cycle (as the frequency of excitation varied) over the frequency range of interest. The obtained data was processed to retain only the maximum points on the velocity curve. These points were then converted into values of displacement using the expression

$$x_{\max} = \frac{v_{\max}}{\omega_d}$$

in which, $x_{\max}$ is the maximum displacement, $v_{\max}$ the maximum velocity and ω_d the damped natural frequency. The transformation assumes the system to vibrate sinusoidally with no damping and is considered to be sufficiently accurate due to the transducers motion being close to sinusoidal, and the low levels of damping present within the system. The resulting amplitude frequency characteristic is shown in Fig. 9. The black curve was obtained as the excitation frequency was swept upwards and the grey curve was obtained as the excitation frequency was swept downwards. It can be seen that there is a small separation between the two

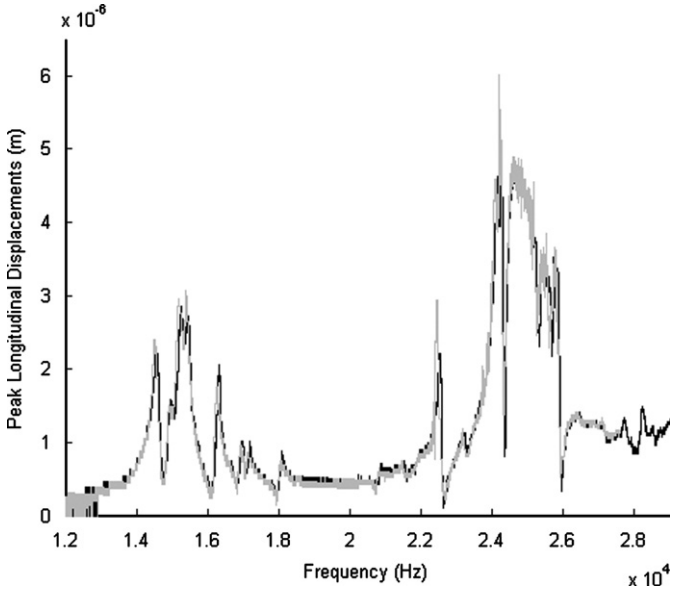

Fig. 9. Amplitude frequency characteristic of free transducer with no drill bit attached.

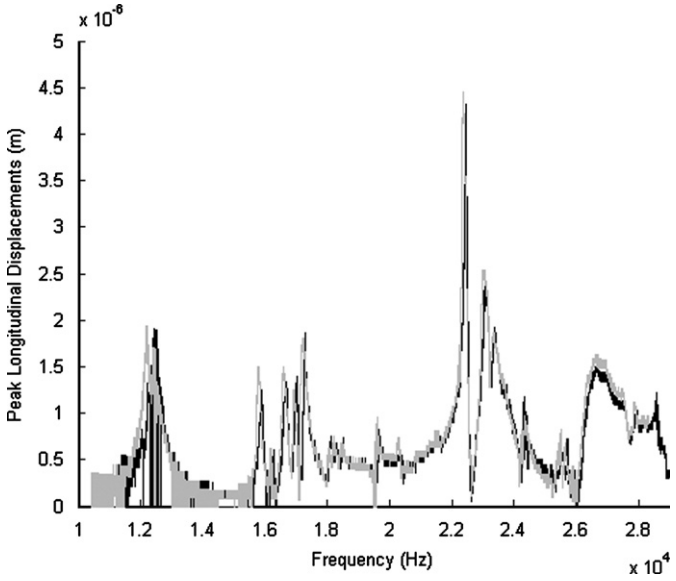

Fig. 10. Amplitude frequency characteristic of free transducer with drill bit attached.

curves but that they are in good agreement; as such, the frequency sweep rate was considered slow enough to reach quasi-static peak amplitudes of vibration throughout the frequency range investigated.

The same experiment was then repeated, but this time with a drill bit installed in the transducer. The results were processed in an identical manner giving the results shown in Fig. 10. Again the black curve relates to the frequency being swept upwards and the grey, downwards. Here, there is also a good agreement between the frequency sweeps. The sharp dips around 12 kHz relate to the laser vibrometer's signal being discontinuous.

A large deviation can be seen between the amplitude frequency characteristic of the transducer with no drill bit attached and that of the transducer with the drill bit attached. This shows the sensitivity of the system to the addition of extra components, and indicates that the complete UAD system should be tuned as a whole [40]; not in parts.

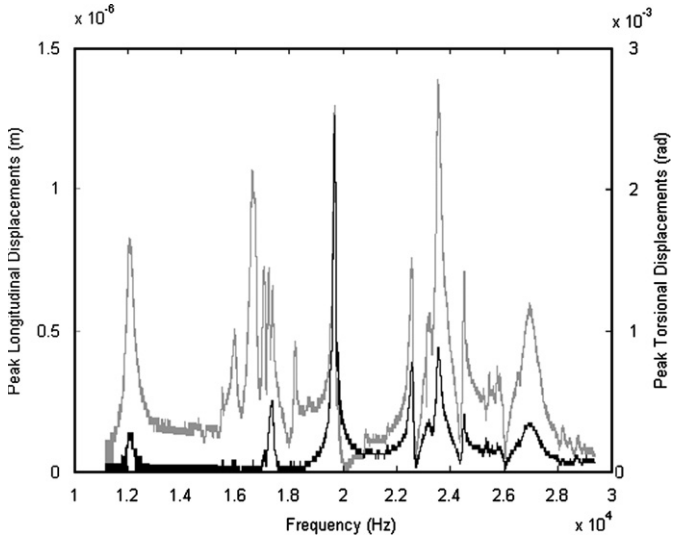

Fig. 11. Amplitude frequency characteristic of the drill bit's tip under purely longitudinal excitation (reduced excitation level).

Further to this, the motion of the drill bit's tip was investigated. Two laser vibrometers were employed, as shown in Fig. 6, and the results were processed in exactly the same manner as for the transducer. Again, it is noted that the level of excitation was reduced slightly during this experiment in order to facilitate data capture. Fig. 11 shows the resulting amplitude frequency characteristic of the drill bit's tip whilst the excitation frequency was being swept upwards. In Fig. 11, the grey curve relates to peak longitudinal displacements and the black curve relates to peak torsional displacements. It must be noted that 3×10^{-3} rad of torsional displacement corresponds to 12 μm of linear displacement at the outer periphery of the drill bit's cutting lip. It is interesting to note, therefore, that in terms of linear displacement at the outer periphery of the drill bit's cutting lip, some points in the curve show approximately seven times the magnitude of linear displacement due to torsional vibration than that for longitudinal displacement. This shows that the helical structure of the drill bit gives rise to a significant level of vibration mode conversion between longitudinal and torsional vibration modes.

The key resonant frequencies exhibited by the transducer in free vibration (with the drill bit attached) are reflected in this characteristic, but with the addition of several other resonant modes that arise due to the drill bit's structure. The curve is also seen to be very peaky, the peaks being extremely sharp and tall. This shows a low level of damping in the vibrating structure, and indicates that instability would occur whilst attempting to maintain resonant vibration using traditional frequency control methods.

The points of maximum vibration of the torsional and longitudinal vibration modes are seen, generally, to coincide, but with differing relative magnitudes. The material's two elastic constants (Young's modulus and shear modulus) differ, which results in two fundamental modes of wave propagation within the body. Consequently, two speeds of wave propagation exist resulting in differing modes of resonance. The drill bit's structure, being helical, couples the two vibration modes, converting longitudinal vibration into torsional vibration and visa versa. When one vibrational mode resonates, vibration mode conversion occurs, and the complementary mode will be excited accordingly. The point of maximum vibration occurring in the complementary mode will be at a reduced level to that of resonance.

Owing to the definition of the data captured, plots can be made that show the relationship between the torsional and longitudinal displacement with respect to time. An example of this data is shown in Fig. 12. Time is shown along the lower right axis and is equal to the delay after the oscilloscope was triggered. The axial displacement of the drill bit's tip is shown up the vertical axis, with positive values denoting the longitudinal extension of the drill bit. Torsional displacement is shown along the lower left axis and positive values occur when the drill bit's tip was twisting clockwise (as viewed from behind the cutting edge) in the direction in which the cutting lips cut. Each relationship shown on the graph (torsional displacement against

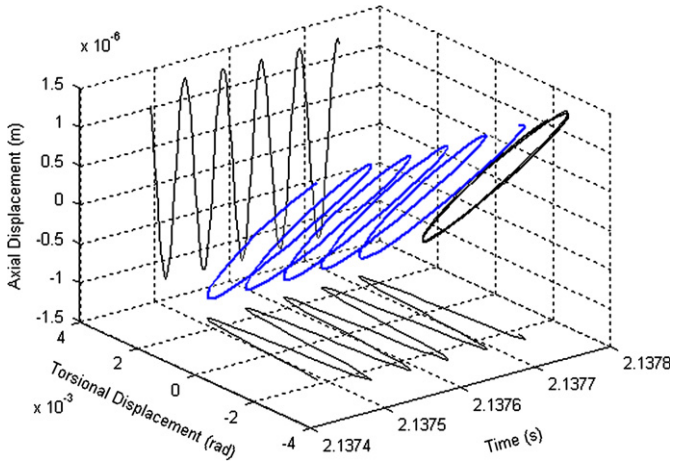

Fig. 12. Vibration locus of the drill bit's tip as measured experimentally.

time, etc.) is shadowed onto the back faces of the graph in order that the data is easier to interpret. This data has been plotted as an example.

3.2. Drilling reaction force and torque measurement

As described previously, the physical arrangement for these experiments was as shown in Fig. 7, and the electrical arrangement was as shown in Fig. 8. The same electrical arrangement that was used to generate the swept sine signal in the free vibration experiments was used during drilling experiments. The excitation voltage was also kept constant (at the larger excitation amplitude).

The oscilloscope was set to trigger from the ramp signal, and as the excitation frequency rose into the range of interest, the charge amplifiers were reset, the oscilloscope was triggered, a small duration prior to cutting was recorded (in order that the charge amplifiers' residual values could be recorded), and cutting was initiated. The excitation signal, torsional reaction, thrust force, and time signature, were recorded simultaneously over a selected duration, and once recorded, the data was transferred to the PC for analysis.

Experiments were repeated in order that average values be obtained. During these experiments, the excitation frequency was swept both upwards and downwards to investigate any influence that this may cause.

Whilst conducting the sweep sine drilling experiments, an effect was noticed that warrants mention. As the workpiece was drilled, chips would often wind themselves inside the flutes of the drill bit. After each test, when chips were still present in the drill's flutes, the lathe's rotation was stopped and the chips were removed manually. It was noticed that, as the swept frequency passed through certain frequencies, the chips would either 'jump' off the drill bit, or would just fall off when gently 'teased'. When no ultrasonic vibration was present, the chips were more difficult to remove. This was observed consistently.

Another observation that was made at certain excitation frequencies was that the drill bit (in free vibration) felt 'oily' to the touch. This is attributed to the motion, caused by ultrasonic excitation, affecting the phenomenological frictional properties of surface–tool interaction.

Once a series of experiments had been conducted with the excitation frequency being swept both upwards and downwards, the data was averaged (for both force and torque) with respect to excitation frequency. The results from this averaging process are shown in Figs. 13 and 14 for torque and thrust, respectively. In these figures, the black curve shows the reactions obtained as the excitation frequency is swept upwards and the grey curves show the reactions when the excitation frequency was swept downwards. The grey horizontal lines show the averaged reactions obtained under conventional drilling conditions i.e. without the use of ultrasound.

Further to the experiments conducted using a swept sine wave excitation, the Black Star signal generator shown in Fig. 8 was substituted for a Time Electronics Ltd. DC Voltage Calibrator (Type 2003S). This device

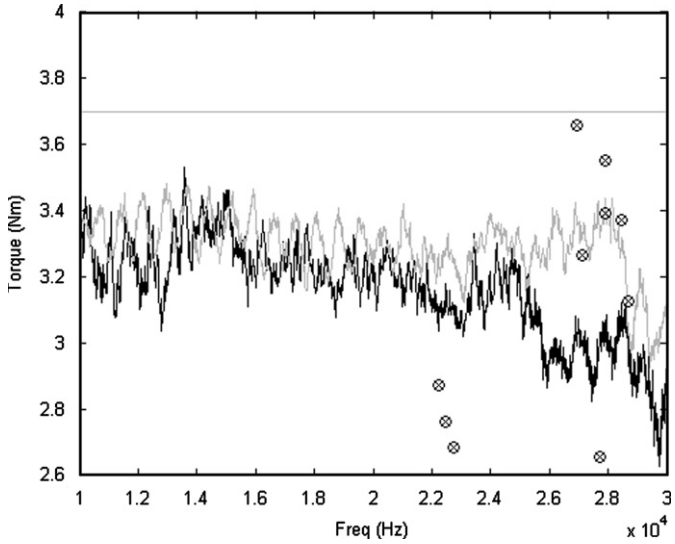

Fig. 13. Relationship between drilling reaction torque and excitation frequency.

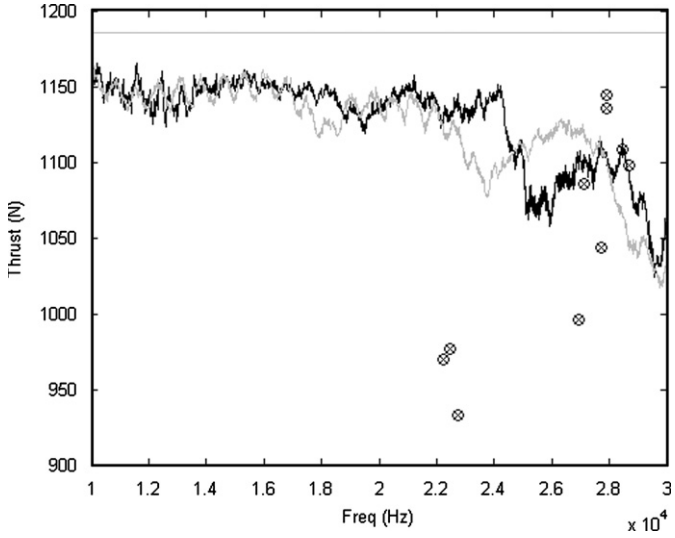

Fig. 14. Relationship between drilling reaction force and excitation frequency.

generates extremely accurate voltages and was used to precisely control the HP generator's VCO input. This resulted in very precise control of excitation frequency.

In addition to the experiments described above, additional experiments were performed to determine the relationships between the drilling reaction forces and the excitation frequency for workpieces that had been predrilled to the thickness of the drill bit's web. The purpose of these experiments was to generate cutting force data to be used subsequently in FE models that incorporate the nonlinear cutting forces that occur during UAD. From the results detailed above, and the additional results obtained from the experiments conducted on pre-drilled workpieces, several optimal excitation frequencies were determined and experiments were conducted under steady state UAD conditions at these frequencies. The reaction torque and force developed during these steady state UAD experiments were averaged, and are included in Figs. 13 and 14 as black crossed circles.

From Figs. 13 and 14, several trends can be deduced. Firstly, the drilling reaction torques and forces developed during UAD are lower than those generated during conventional drilling throughout the frequency

range investigated. Both the torque and the force curves show optimal positions, relating to differing excitation frequencies, at which minimal force/torque reactions occur. These optimal positions often coincide in both the torque and force curves indicating that the UAD process is more efficient at these excitation frequencies. The drilling torque and force reactions that occur as the excitation frequency is swept downwards deviate strongly from those measured as the frequency is swept upwards indicating that the vibration system is strongly effected by prior cutting events and that the speed at which the frequency is swept is not sufficiently slow to reach quasi-steady-state UAD conditions. This is further confirmed by the results obtained from steady-state UAD experiments in which the average drilling reactions measured deviate greatly from those obtained during swept excitation experiments.

4. FE model

Owing to the complexity of vibration propagation, reflection, and dissipation in helical structures, analytical methods become arduous if feasible to employ. For this reason, a generic FE model was developed that could be employed to predict vibration characteristics of complex ultrasonic structures.

4.1. Model development

Three-dimensional CAD data for the drill bit under test was acquired from the drill bit's manufacturer. This data was subtly simplified (without significantly influencing its vibration properties) in order to assist in mesh generation. The meshed geometry of the drill bit is shown in Fig. 15.

An implicit time domain FE model was developed which modelled the drill bit's material with respect to its elastic and inertial properties. The field equations of motion that describe the displacements due to three-dimensional wave propagation in isotropic, homogeneous solids that are subjected to negligible body forces and are under small displacement conditions can be written as [41]

$$\rho\frac{\partial^2\mathbf{u}_i}{\partial t^2}=(\lambda+\partial)\frac{\partial \Delta}{\partial \mathbf{x}_i}+\mu\frac{\partial^2\mathbf{u}_i}{\partial x_j\partial \mathbf{x}_j},\quad i=j=1,2,3,$$

where ρ is the density, $\mathbf{u}_i$ the displacement, t the time, λ and μ are Lamé's material constants, $\mathbf{x}_i$ and $\mathbf{x}_j$ indicate the directions in which the derivatives are calculated, and Δ the dilatation,

$$\Delta=\boldsymbol{\varepsilon}_{ii}.$$

This formulation was modified in order to introduce internal material damping. The drill bit's material was assumed to behave as a Kelvin–Voight solid, and both of the elastic constants were complemented with viscous equivalents in order that the damping within the material that related to the two modes of wave propagation (longitudinal and shear) could be assigned independently. This model of damping assumes that the internal material losses are directly proportional to velocity and is assumed to be sufficiently

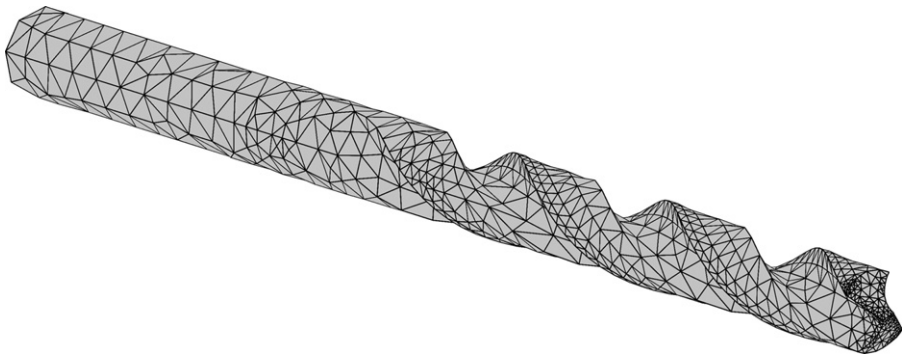

Fig. 15. The meshed finite element geometry of the drill bit under test.

accurate within the frequency range and vibration amplitudes considered. The modified formulation can be written as

$$\rho\frac{\partial^2\mathbf{u}_i}{\partial t^2}=(\lambda+\mu)\frac{\partial \Delta}{\partial \mathbf{x}_i}+\mu\frac{\partial^2\mathbf{u}_i}{\partial \mathbf{x}_j\partial \mathbf{x}_j}+\left(b_\lambda+b_\mu\right)\frac{\partial \dot{\Delta}}{\partial \mathbf{x}_i}+b_\mu\frac{\partial^2\dot{\mathbf{u}}_i}{\partial \mathbf{x}_j\partial \mathbf{x}_j},\quad i=j=1,2,3,$$

where b_λ relates to the elastic constant λ, and b_μ relates to the elastic constant μ. A small dot above a symbol denotes derivative with respect to time.

The drill bit model was orientated so that its central axis (along its length) coincided with the $\mathbf{x}_1$-axis.

Two forms of boundary condition were employed in the FE model. The first was a direct constraint of the dependant variable $\mathbf{u}_i$ (displacement). This condition was used to constrain a line implanted within the drill bit, and along its central axis i.e. along the axis $\mathbf{x}_1$. The constraint acts in the 2 and 3 directions i.e. $\mathbf{u}_2=\mathbf{u}_3=0$. This prevented any transverse bending to occur along the length of the drill bit but allowed for both longitudinal and torsional displacements. The drill bit model was excited in the same position as that during experimental investigations. This is shown in Fig. 6 by the ring around the drill bit's shaft. The transducer end's velocity, which was obtained during experimental investigations, was integrated numerically and the low-frequency vibration components were filtered out to give the displacement at the end of the transducer during free vibration (with the drill bit attached). These displacement values $f(t)$ were then used to excite the drill bit model (due to the varying amplitude frequency response of the transducer employed) in order to allow a direct comparison between experimental results and those obtained from FE analysis. As such, the drill bit's boundary, at which the excitation was applied, was subjected to the condition $\mathbf{u}_1=f(t)$. This condition also prevented solid body motion in the $\mathbf{x}_1$ direction. Finally, the boundary at which the transducer was attached (again, the ring around the drill bit's shaft in Fig. 6) was constrained torsionally to prevent solid body rotation but allowed to expansion and contract i.e. $(\mathbf{u}_3/\mathbf{u}_2)=(\mathbf{x}_3/\mathbf{x}_2)$.

The second form of boundary condition was applied to all remaining boundaries of the drill bit and allowed free vibration. The boundary condition can be written as

$$\mathbf{n}_i\bullet\left((\lambda+\mu)\frac{\partial \Delta}{\partial \mathbf{x}_i}+\mu\frac{\partial^2\mathbf{u}_i}{\partial \mathbf{x}_j\partial \mathbf{x}_j}+\left(b_\lambda+b_\mu\right)\frac{\partial \dot{\Delta}}{\partial \mathbf{x}_i}+b_\mu\frac{\partial^2\dot{\mathbf{u}}_i}{\partial \mathbf{x}_j\partial \mathbf{x}_j}\right)=0,\quad i=j=1,2,3,$$

where $\mathbf{n}_i$ is a unit vector normal to the surface of the boundary.

The model described accounts for both longitudinal and torsional modes of wave propagation and the vibration mode conversion that occurs as a result of the drill bit's helical structure. The equations of motion were solved using the principle of virtual work.

The internal damping present within HSS was measured experimentally by impacting tuned (for frequency) cylindrical samples, to a displacement amplitude of approximately 3.5 μm, and measuring the decaying vibration. From these experiments, the damping present within the material could be characterised using two values of quality factor, one for shear or torsional vibration, the other for longitudinal or extensional vibration. These were found to be $Q_{\text{Shear}}=18{,}000$ and $Q_{\text{Long}}=19{,}000$, respectively. Due to the complexity of decoupling the vibrating samples from their immediate environment, these values are assumed to be conservative.

As it is not feasible to model such low levels of damping in time domain FE numerical models (with reasonable computational resources), quality factors of $Q=250$ were selected for both longitudinal and torsional vibration modes. This is justified as previous investigations at Loughborough University have determined these values as being representative of complete transducer/cutting tool systems. These damping levels exhibit pronounced resonant characteristics but they are not overly computationally strenuous. The damping coefficients employed were derived iteratively from FE models of simple bars that were tuned to oscillate in free vibration at the frequencies of interest. The geometries of these models were that of the experimental samples used, and they were also employed to fine-tune the material's elastic constants.

The drill bit model was started from a resting condition (i.e. no vibration present) and any frictional contact between the inside of the transducer and the cylindrical surface of the drill bit's shaft was neglected (this was assumed to be incorporated into the increased internal material damping). The resulting vibration of the drill

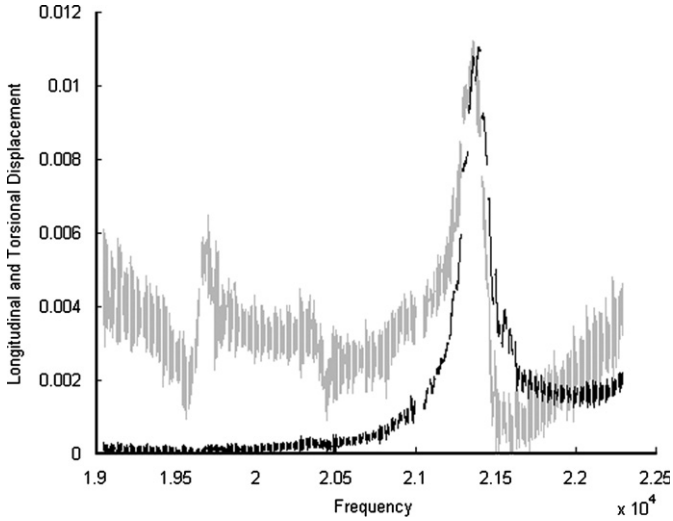

Fig. 16. Amplitude frequency characteristic of the drill bit's tip as derived numerically.

bit's tip (both longitudinal and torsional) was averaged over the surface of the drill tip's face in order to obtain consistent results and reduce numerical error.

4.2. FE results and discussion

The numerical results obtained from swept sine wave excitation using experimentally measured displacements were exported and processed in an identical manner to that of the experimentally measured data. The peak vibration displacements for both longitudinal and torsional vibration were isolated and are plotted in Fig. 16. The grey curve relates to the characteristic of longitudinal vibration, and the black, torsional. The damping used in the FE model was far higher than that exhibited by HSS. This fact renders the numerical values obtained from FE qualitative, not quantitative. It will also affect the sharpness of resonant curves. Furthermore, a scaling factor was used to plot both the longitudinal and torsional results against the same axis.

The curve is seen to oscillate and is discontinuous in places because many simulations were run in order to compile the data. In each simulation, the drill bit was allowed to reach steady state, and was then analysed further for a period of time. The simulations were overlapped with respect to time so that a complete picture could be assembled. Only the steady-state data is included in the plot. The simulation was run from experimental data (measured from the transducer's tip) in which the excitation frequency was swept upwards (at the higher excitation level).

As was the case for the experimental results, sufficient data was generated in order to plot the torsional and longitudinal displacement of the drill bit's tip with respect to time. Plots similar to Fig. 12 can be created to investigate vibration mode conversion and to identify the numerical data with that obtained from experimentation.

5. Comparison between FE and experimental results, and general discussion

The numerically derived amplitude frequency characteristic presented in Fig. 16 shows a frequency shift when compared to the experimentally measured data shown in Fig. 11. The numerical results relate to the experimental results in the approximate frequency range 17.6–20.5 kHz. This is assumed to be a result of the elastic coefficients in the FE model being inaccurate. The FE model's elastic coefficients were derived by comparing numerical results to the results obtained by experimental analysis of cylindrical bars. The drill bit manufacturer provided the cylindrical bars under test (i.e. they were of the same material as the drill bit), but their material may have been in a differing metallurgical condition (due to the fact that they were solid cylinders) to the drill bits under test. The shapes of the amplitude frequency relationships for both longitudinal and torsional vibration show a good resemblance between

the experimentally measured and numerically calculated data. The numerically derived curves are seen to almost exactly trace the shape of the experimentally measured data. This indicates that the FE model can be effectively employed to analyse vibrating drill structures.

Further analysis will be performed investigating the drill bit tip's displacement locus at different excitation frequencies. Correlations between the experimental and numerical data will be further investigated.

Although on initial inspection the FE model shows good similarities with experimental results, during drilling, the forces that act on the drill bit will vary according to the motion of the drill bit's cutting edges and surfaces. These forces will affect the motion of the drill bit and the history of the cuts performed on the workpiece (as was proven with the experimental drilling results) will further influence the reaction forces. In order to address this, a cutting model is required that retains information regarding the previous cuts performed.

The workpieces drilled during the drilling experiments have been retained. Physical characteristics of cut surfaces can reveal a great deal about the efficiency and accuracy of the cutting process. Further analysis will reveal more information about the UAD experiments conducted.

It must be noted that throughout the experiments documented in this work, the excitation signal was generated using conventional signal generators. Previous research at Loughborough University [42–44], and independently in Taiwan [17], has proven that autoresonant control can be effectively employed to stabilise ultrasonic vibrating systems that are subjected to varying nonlinear loadings. Autoresonant control uses phase control methods rather than traditional frequency control methods to maintain optimum vibration levels within a system; the resulting control loop is far more stable. This work will ultimately result in an optimised physical vibration structure for UAD and will employ autoresonant control.

6. Conclusions

The drill bit considered displayed strong vibration mode conversion characteristics during both experimentation and numerical simulation. Its amplitude frequency response curve is also extremely peaky, indicating instability when controlled using traditional frequency control methods.

Although the damping levels employed in the numerical model are far higher than those measured experimentally, the characteristics obtained from the numerical model (in form) are seen to accurately reflect those measured experimentally.

The cutting mechanism of a drill bit must be considered when designing and optimising UAD systems. Current UAD systems are in no way optimised. Further investigation, both experimental and numerical, is required to develop a vibrating system that exhibits a stable and kinematically beneficial vibratory motion.

The nonlinear drilling reaction forces encountered whilst drilling, and their effect on the ultrasonic system, need to be quantified and addressed. The drilling reaction forces are also seen to be strongly dependant on prior cutting events.

References

[1] C.J. Oxford, On the drilling of metals 1—basic mechanics of the process, *Transactions of the ASME* 77 (1955) 103–114.
[2] E.P. DeGarmo, J.T. Black, R.A. Kohser, *Materials and Processes in Manufacturing*, ninth ed., Wiley, New York, 2003.
[3] Z. Linbo, W. Lijiang, W. Xin, Study on vibration drilling of fiber reinforced plastics with hybrid variation parameters method, *Composites: Part A* 34 (2003) 237–244.
[4] K. Adachi, N. Arai, K. Okita, S. Wakisaka, F. Kuratani. Study on burr in low frequency vibratory drilling, *Proceedings of the Fifth International Conference on Production Engineering* (conference code 10402), Japan Society of Precision Engineering, Tokyo, Japan, 1984.
[5] K. Adachi, N. Arai, S. Harada, K. Okita, S. Wakisaka, Study on burr in low frequency vibratory drilling—drilling of aluminum, *Bulletin of the Japan Society of Precision Engineering* 21 (4) (1987) 258–264.
[6] K.F. Graff, Macrosonics in industry 5: ultrasonic machining, *Ultrasonics* 13 (3) (1975) 103–109.
[7] H. Takeyama, S. Kato, Burrless drilling by means of ultrasonic vibration, *CIRP Annals* 40 (1) (1991) 83–86.
[8] H. Onikura, O. Ohnishi, J. Feng, T. Kanda, T. Morita, Effects of ultrasonic vibration on machining accuracy in microdrilling, *International Journal of the Japan Society for Precision Engineering* 30 (3) (1996) 210–216.
[9] D.-Y. Zhang, X.-J. Feng, W. Zhang, D.-C. Cheng, Study on the drill skidding motion in ultrasonic vibration microdrilling, *American Society of Mechanical Engineers, Production Engineering Division (Publication) PED* 55 (1991) 361–371.

[10] H. Suzuki, H. Yagishita, Burrless drilling by vibration cutting applying ultrasonic torsional mode vibration, *Transactions of the NAMRC/SME* 33 (2005) 2005–2199.
[11] S.S.F. Chang, G.M. Bone, Burr size reduction in drilling by ultrasonic assistance, *Robotics and Computer-Integrated Manufacturing* 21 (4–5) (2005) 442–450.
[12] S.S.F. Chang, *Ultrasonic assisted machining*, 2004. 〈http://mmri.eng.mcmaster.ca/mmri/posters/chang04.pdf〉.
[13] G. Deng, S. Li, S. Wu, X. Yang, Ultrasonic vibration drilling of small-diameter deep holes of difficult-to-machine stainless steel: theoretical analysis and comparative experimental research, *American Society of Mechanical Engineers, Production Engineering Division (Publication) PED* 64 (1993) 835–839.
[14] J. Devine, *Ultrasonically Assisted Metal Removal. American Society for Metals*, Fabrication of Composite Materials: Source Book, 1985, pp. 329–334.
[15] J. Huber, Ultrasonic drilling (application to titanium machining in aircraft production), *Materials and Processes for the 70's—Cost Effectiveness and Reliability*, 1973, pp. 28–42.
[16] D.-y. Zhang, X.-j. Feng, L.-j. Wang, D.-c. Chen, Study on the drill skidding motion in ultrasonic vibration microdrilling, *International Journal of Machine Tools & Manufacture* 34 (6) (1994) 847–857.
[17] Y.C. Chen, Y.S. Liao, J.D. Fan, Autoresonant tuning and control in ultrasonic vibration assisted drilling process, *Materials Science Forum* 505/507 (2) (2006) 823–828.
[18] R. Neugebauer, A. Stoll, Ultrasonic application in drilling, *Journal of Materials Processing Technology* 149 (1–3) (2004) 633–639.
[19] Anon, Ultrasonically assisted gun drilling, *Cutting Tool Engineering* 33 (9–10) (1981) 24–28.
[20] A. Shoh, New look at ultrasonic metal drilling, *SAMPE Quarterly* 1 (4) (1970) 11–16.
[21] H.V. Fairbanks. Ultrasonic assist in drilling of metals and in molding of polymer powders, *Proceedings of the 27th International Conference on Production Engineering*, New Delhi, India, 1977.
[22] C.S. Liu, B. Zhao, G.F. Gao, X.H. Zhang, Study on ultrasonic vibration drilling of particulate reinforced aluminium matrix composites, *Key Engineering Materials* 291/292 (2005) 447–452.
[23] S. Aoki, S. Hirai, T. Nishimura, Prevention from delamination of composite material during drilling using ultrasonic vibration, *Key Engineering Materials* 291/292 (Advances in Abrasive Technology VIII) (2005) 465–470.
[24] N. Ahmed, A.V. Mitrofanov, V.I. Babitsky, V.V. Silberschmidt, Analysis of material response to ultrasonic vibration loading in turning inconel 718, *Materials Science and Engineering A* 424 (1–2) (2006) 318–325.
[25] A.V. Mitrofanov, V.I. Babitsky, V.V. Silberschmidt, Finite element simulations of ultrasonically assisted turning, *Computational Materials Science* 28 (3–4) (2003) 645–653.
[26] A.V. Mitrofanov, V.I. Babitsky, V.V. Silberschmidt, Finite element analysis of ultrasonically assisted turning of inconel 718, *Journal of Materials Processing Technology* 153–154 (2004) 233–239.
[27] S. Aoki, T. Nishimura, Prevention of delamination during drilling of composite material using vibration, *Key Engineering Materials* 261/263 (1) (2004) 381–386.
[28] M. Iwai, T. Goutani, T. Uematsu, K. Suzuki, K. Tanaka, Application of megasonic coolant to drilling process, *Seventh International Symposium on Advances in Abrasive Technology*, Bursa, Turkey, 2004.
[29] C.X. Ma, E. Shamoto, T. Moriwaki, Drilling assisted by ultrasonic elliptical vibration, *Key Engineering Materials* 291–292 (2005) 443–446.
[30] A.I. Markov, *Ultrasonic Machining of Intractable Materials*, Iliffe Books Ltd., London, 1966.
[31] J. Kumabe, *Vibration Assisted Cutting—Basics and Applications*, Jikkyo Shuppan Co. Ltd., Tokyo, 1979 (in Japanese).
[32] HNI, *Heinz Nixdorf Institute within the University of Paderborn together with the Institute for Machine Tools at the University of Stuttgart*, 2007. 〈http://wwwhni-alt.upb.de/projekte/projekt_e.php3?id=343〉.
[33] O. Ohnishi, H. Onikura, A. Hata, K. Yamamoto, Fabrication of micro flat drills by precision grinding and drilling into duralumin and stainless steel with ultrasonic vibration, *JSME International Journal, Series C: Mechanical Systems, Machine Elements and Manufacturing* 47(1) (2004) 117–122.
[34] K. Egashira, K. Mizutani, T. Nagao, Ultrasonic vibration drilling of microholes in glass, *CIRP Annals* 51 (1) (2002) 339–342.
[35] A. Shoh, New developments in metal working processes, *Journal of the Acoustical Society of America* 52 (1A) (1972) 134.
[36] Fuji, *Fuji ultrasonic engineering*, 2006 〈http://www.fuji-us.co.jp/e/index.html〉.
[37] M. Anon, Cutting and milling system utilizing ultrasonic vibrations, *New Technology Japan* 28 (12) (2001) 35.
[38] A. Shoh, Industrial applications of ultrasound—a review: 1. High-power ultrasound, *IEEE Transactions on Sonics and Ultrasonics* SU-22 (2) (1975) 60–71.
[39] A. Mari, Grumman widens ultrasonic, laser use, *American Metal Market—Metalworking News* 80 (172) (1973) 1–5.
[40] V.I. Babitsky, A. Meadows, V.K. Astashev, Vibration excitation and energy transfer during ultrasonically assisted drilling, *Journal of Sound and Vibration* (2006), in press.
[41] R.J. Wasley, *Stress Wave Propagation in Solids—An Introduction*, Marcel Dekker, Inc., New York, 1973.
[42] V.I. Babitsky, V.K. Astashev, A.N. Kalashnikov, Autoresonant control of nonlinear mode in ultrasonic transducer for machining applications, *Ultrasonics* 42 (1–9) (2004) 29–35.
[43] V. Babitsky, V. Astashev, Nonlinear dynamics and control of ultrasonically assisted machining. *Proceedings of the ASME International Design Engineering Technical Conferences and Computers and Information in Engineering Conference—DETC2005*, Vol. 1A, 2005, pp. 747–754.
[44] V.I. Babitsky, A.N. Kalashnikov, F.V. Molodtsov, Autoresonant control of ultrasonically assisted cutting, *Mechatronics* 14 (1) (2004) 91–114.